ACS APPLIED MATERIALS & INTERFACES

Research Article

www.acsami.org

Graphene Surface Plasmon Induced Optical Field Confinement and Lasing Enhancement in ZnO Whispering-Gallery Microcavity

Jitao Li,[†] Chunxiang Xu,*[,†] Haiyan Nan,[‡] Mingming Jiang,[§] Guangyu Gao,[⊥] Yi Lin,[†] Jun Dai,[†] Gangyi Zhu,[†] Zhenhua Ni,[‡] Shufeng Wang,[⊥] and Yan Li[⊥]

[†]State Key Laboratory of Bioelectronics, School of Biological Science and Medical Engineering, and [‡]Department of Physics, Southeast University, Nanjing 210096, China

[§]State key Laboratory of Luminescence and Applications, Changchun Institute of Optics, Fine Mechanics and Physics, Chinese Academy of Sciences, Changchun 130033, China

[⊥]Institute of Modern Optics & State Key Laboratory for Mesoscopic Physics, School of Physics, Peking University, Beijing 100871, China

ABSTRACT: Fundamental physics under the surface plasmon (SP) of graphene and the functional application beyond ultraviolet (UV) lasing of ZnO are both fascinating research areas. Herein, the optical field confinement induced by graphene SP was simulated theoretically in a graphene-coated ZnO microrod, which acted as a whispering-gallery microcavity for lasing resonance. Distinct optical field confinement and photoluminescence (PL) enhancement were observed experimentally. Stable and transient spectra were employed to analyze the PL enhancement and the coupling dynamics between graphene SP and ZnO interband emission. As a functional application, the graphene-coated ZnO microcavities presented the obviously improved whispering-gallery mode (WGM) lasing performance. These results would be valuable for designing novel optical and photoelectronic devices based on SP coupling in graphene-semiconductor hybrid materials.

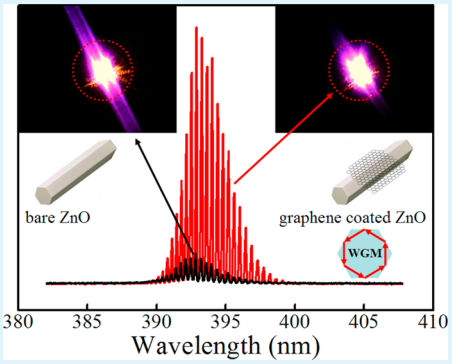

KEYWORDS: *graphene, ZnO, surface plasmon, optical field confinement, whispering-gallery mode lasing*

1. INTRODUCTION

Surface plasmon (SP) is a spatially confined electromagnetic field originating from the collective oscillation of free electrons at the metal/semiconductor or dielectric interfaces.[1,2] Noble metals have been widely regarded as the best available plasmonic materials for the improved photonic applications, such as surface enhanced Raman scattering,[3−6] light harvesting,[7,8] and optical nanoantenna.[9] The metal SP coupling with semiconductors has been demonstrated as an effective approach to improve the quantum efficiency of light emitting materials and devices.[10−13] However, the metal SP is inconveniently tunable in devices and generally has large Ohmic losses,[14−17] which astricts the flexible design and development of novel functional photonic materials and devices with high performance.

Recent researches have predicted that graphene has an extremely high quantum efficiency for light-matter interaction and strong plasmons based on its unique honeycomb lattice structure and the corresponding Dirac-type energy band.[18] Graphene is expected as a plasmonic material alternative to the noble metals in certain extent, and even with better behaviors because of the two-dimensional nature of the collective excitations. So far, both theoretical and experimental researches have demonstrated the SP of pristine and doped graphene with relatively low loss, high confinement, flexible and tunable features. However, the research on graphene SP is mainly concentrated on the THz region;[19−21] its response in the UV region is lacking in both physical understanding and experimental realization.

ZnO has been recognized as a competent candidate for short wavelength photoelectronic devices, especially for UV lasers, based on its wide direct bandgap of 3.37 eV and large exciton binding energy of 60 meV. A series of previous reports have demonstrated the high quality factor and low threshold of ZnO WGM lasing,[22−26] and laid out the great significance to further improve the lasing performance. As an effective approach to improve light emission of semiconductors, SP of Au and Ag have been employed to enhance the UV spontaneous and stimulated emission of ZnO.[27−29] Though a few reports have observed PL enhancement from the graphene-coated ZnO and assumed the action of graphene SP,[30−32] the mechanism is unclear, even in some controversy. Theoretical simulation and direct visualization of the propagating and confinement behavior of graphene SP are really needed to support the assumed SP effect at the interface of graphene/ZnO. It is of great significance not only to improve the UV emission in

Received: April 3, 2014
Accepted: June 20, 2014
Published: June 20, 2014

phenomenon but also to understand the generation and coupling process of graphene SP in essence, as well as to design novel optical and photoelectronic devices through the investigation on the interaction between graphene SP and ZnO interband emission. More advantageously and importantly, the evanescent wave near the whispering-gallery microcavity surface provides a favorable physical domain for SP coupling, especially for the flat and flexible graphene-coated case, which is expected to effectively improve the WGM lasing performance.

In this paper, optical field confinement and PL enhancement induced by graphene SP were investigated in theory and were also observed intuitively in experiment in a monolayer graphene-coated ZnO whispering-gallery microcavity. The time-resolved photoluminescence (TRPL) experiment was carried out to reveal the coupling dynamics between graphene SP and ZnO interband emission. As a functional application, the graphene SP obviously induced improvement of the ZnO WGM lasing performance. The results are helpful not only to understand the interaction between graphene and semiconductor under the optical excitation in physics but also to inspire novel design of graphene-based optical and photoelectronic devices in technology.

2. EXPERIMENTAL SECTION

The ZnO microrods were synthesized by a vapor phase transport (VPT) method similar to our previous reports.[33] Briefly, a mixture of ZnO and graphite powders with definite mass ratio of 1:1 was filled into a quartz boat as source materials, and a Si substrate was covered on the quartz boat, which was inserted into a horizontal tube furnace. The furnace was then heated up to 1150 °C and maintained at this temperature. The ZnO microrods were obtained on the Si substrate after growing for 45 min.

The monolayer graphene was synthesized by chemical vapor deposition (CVD) method.[34] The graphene was grown on thin copper foils (25 μm) at 1045 °C with a flow of H_2 (60 sccm) and CH_4 (90 sccm). The growth pressure was 320 Pa and growth time was 10 min.

After growth of the ZnO microrods, an individual ZnO microrod was picked out and put onto a SiO_2/Si substrate to construct a whispering-gallery microcavity under an optical microscope. For comparison, three types of microcavities were fabricated. Type I was the bare ZnO microrod. Type II microcavity was fabricated by transferring the type I microrod on a monolayer graphene coated SiO_2/Si substrate. After that, another piece of monolayer graphene was transferred onto the type II microcavity to fabricate the type III microcavity.

The morphology of the sample was characterized by optical microscope (OLYMPUS BX53F), field-emission scanning electron microscope (FESEM, Carl Zeiss Ultra Plus). Raman spectra were recorded on a Lab RAM HR 800 micro-Raman system with 514.5 nm excitation. The micro-PL mapping was done at the same equipment with a He−Cd laser at 325 nm as excitation source. TRPL experiments were performed by an optically triggered streak camera system (C5410, Hamamatsu) at 295 nm from frequency doubling of the fundamental 120 fs pulses at 590 nm with a repetition rate of 76 MHz (Mira OPO, Coherent). For WGM lasing measurements, the bare ZnO microrod and the hybrid microcavities were excited by focused 325 nm femtosecond pulse laser. The lasing spectra were measured by a micro-PL system and the data was collected by an optical multichannel analyzer (Princeton, Acton SP2500i), the spectral resolution of the spectrometer is 0.025 nm, the optical images were captured by a camera linked to this measurement setup. All measurements were performed at room temperature. Theoretical calculation and simulations were carried out using finite difference time domain (FDTD) method.

3. RESULTS AND DISCUSSION

The proposed hybrid microcavity is schematically shown in Figure 1, where a piece of monolayer graphene was coated on a

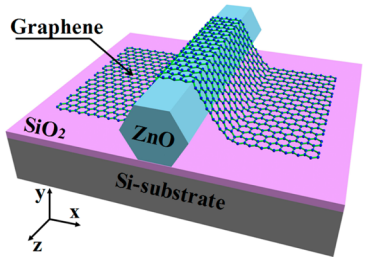

Figure 1. Schematic diagram of the graphene-coated ZnO microrod hybrid microcavity.

ZnO microrod, which has perfect hexagonal cross section and smooth side surfaces. This hybrid structure sets a configuration for plasmon generation and coupling with ZnO emission, and further acts as whispering-gallery microcavity for stimulated resonance.

An individual ZnO microrod put on a SiO_2/Si substrate was employed to simulate the WGM lasing behavior, where the corresponding refractive index was selected as n_{air} = 1.0, n_{ZnO} = 2.45, and n_{SiO_2} = 1.5. Figure 2a shows the electric field energy distribution in the $x-y$ plane of the bare ZnO microrod. It can be found that the electric field is well confined within the ZnO microrod due to the totally internal reflection at the inner walls to form the whispering-gallery modes. To explore the light propagation in the bare ZnO microrod, three-dimensional distribution of the electric field has also been simulated. The patterns shown in Figure 2b, c demonstrate obvious energy oscillation inside the microrod along the z direction, accompanied by obvious attenuation. This simulation result is consistent with the experimental observation, which will be discussed later, and shows that the emission light can propagate a certain distance along the z direction with proper optical loss.

As a simplified model, the graphene coated top surface of the ZnO microrod was derived from the hybrid microcavity to simulate the coupling interaction between graphene and ZnO, as shown the sandwich structure in Figure 3a.

For simulation, the parameters were chosen as the carrier density $n \approx 1 \times 10^{13}$ cm^{-2}, the relaxation time corresponds to DC mobility $\mu = 1 \times 10^4$ cm^2/(V s) and the Fermi energy E_F = 0.375 meV according to previous reports.[30,35] Figure 3b shows the evanescent field distribution for fundamental, second-order and third-order eigenmodes, and corresponding field intensities along the x-axis of the interface between graphene and ZnO. The simulation results clearly demonstrate that the SP effectively generate at the interface of graphene/ZnO and is highly confined in the ZnO microcavity. This indicates the coupling between graphene SP and ZnO emission, and supports the experimental observation on the confinement and enhancement of the light emission from the whispering-gallery microcavity. On the basis of this confinement effect of graphene SP, the emission light could be highly confined in a small excited spot when the graphene-coated ZnO microcavity is irradiated by UV laser. This is different from the attenuation phenomenon in the bare microrod, and supports the experimental observation on the confinement and enhancement of the light emission from the WGM microcavity as disscussed later.

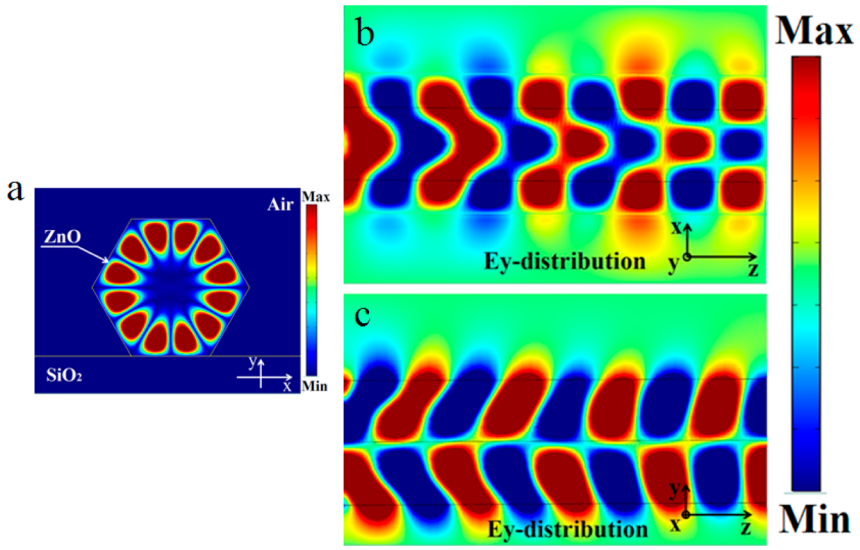

Figure 2. (a) Electric field energy distribution in $x-y$ plane of a bare ZnO microrod placed on a SiO_2/Si substrate. (b, c) y component of the electric field, Ey, distribution in (b) the $x-z$ plane and (c) the $y-z$ plane of the bare ZnO microrod.

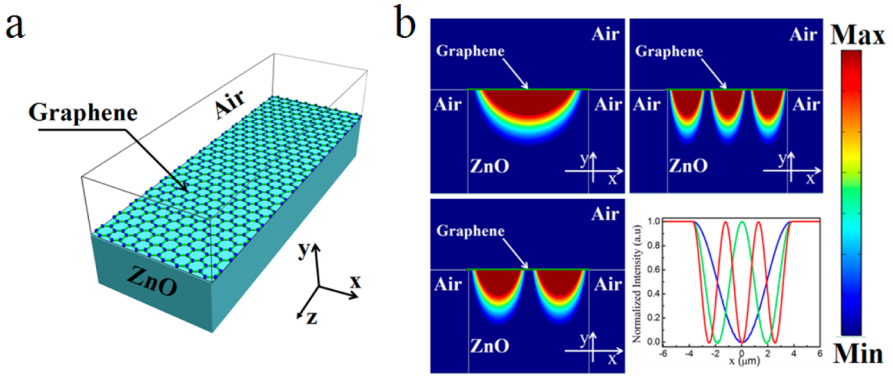

Figure 3. (a) Dissociated model of the hybrid microcavity at the interface of air/graphene/ZnO. (b) Evanescent field distribution of first, second and third order eigenmodes of graphene SP in $x-y$ plane of the graphene-coated ZnO microrod and the corresponding field intensities along the x-axis of the interface between graphene and ZnO. The blue, green and red line demonstrate the field intensity of first, second, and third eigenmode, respectively.

Figure 4a shows the SEM image of the ZnO microrods grown on Si substrate. The microrods present 5−20 μm in diameter and 5−10 mm in length. An enlarged SEM image of an individual ZnO microrod is inserted in Figure 4a, displaying a perfect hexagonal cross-section and flat side surfaces. The PL spectrum of the ZnO microrods at low excitation power is shown in Figure 4b, which illustrates a strong UV emission band at 388 nm from the interband exciton recombination and a very weak green band related to defects. The perfect hexagonal morphology and the strong UV emission indicate that the ZnO microrod is favorable to act as a whispering-gallery microcavity for UV lasing.

The monolayer graphene used in this experiment was synthesized by chemical vapor deposition (CVD) method, and Raman spectroscopy was employed to identify its quality.[36] As shown in Figure 4c, the sharp 2D and G peaks present the single-Lorentzian curves with the full width at half-maximum (fwhm) of 31 and 19 cm^{-1}, respectively. The intensity ratio of 2D mode to G mode (I_{2D}/I_G) is about 2.5, indicating the high quality of the monolayer graphene.[37] Raman spectrum of the ZnO microrod shown in Figure 4d reveals the scattering peaks at 437, 380, and 407 cm^{-1}, corresponding to the typical optical modes of E_2(high), A_1(TO), and E_1(TO) of wurtzite ZnO, respectively.[38] The strong E_2 mode demonstrates the good crystal quality of the ZnO microrods.

As the graphene-coated ZnO microrod was excited by UV laser, an obvious optical field confinement was observed distinctly. Panels a and b in Figure 5 compare the optical images of the same ZnO microrod before and after graphene covering under the same excitation condition. As shown in Figure 5a, the bare ZnO microrod emits bright light, where the bright spot corresponds to the incident position. It can be seen clearly that a small part of the light leaks out of the excited region and propagates a proper distance along the microrod with obvious radiation losses, which is consistent with the simulation results for the bare ZnO microrod discussed in Figure 2. Whereas, as shown in Figure 5b, when the graphene-coated ZnO microrod was excited under the same experimental condition, it emits out much brighter dazzling light, and the emission light was almost confined in the excitation spot. These optical field confinement and enhancement phenomena agree well with the simulation results discussed above, and can be attributed to the graphene SP contribution.

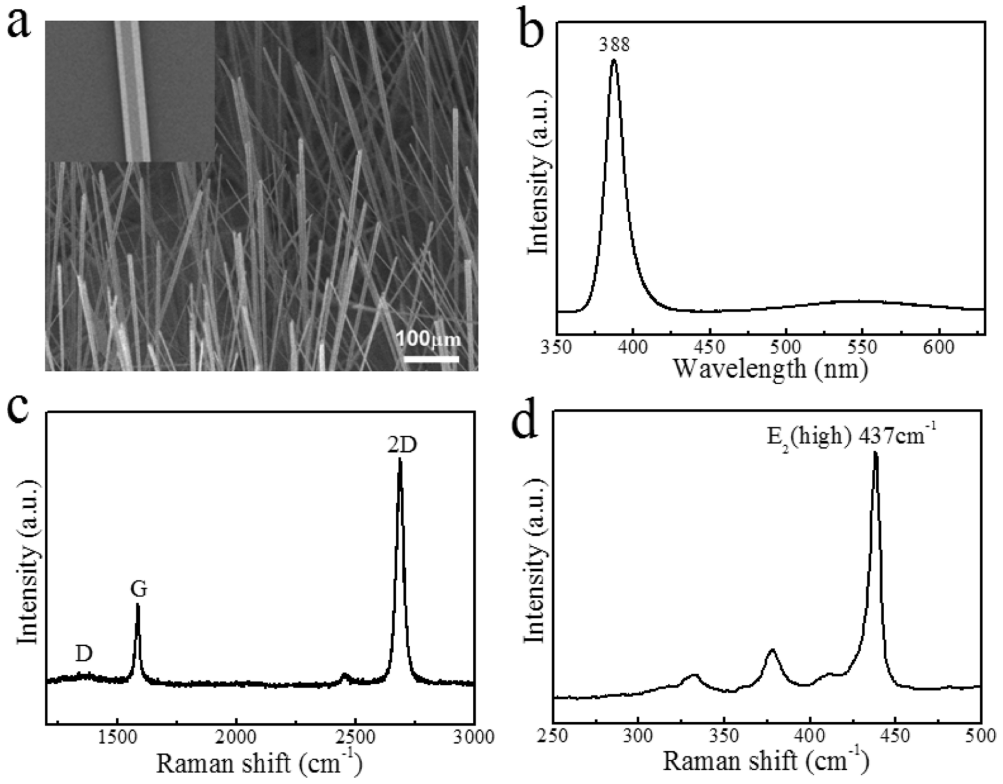

Figure 4. (a) SEM image of as-grown ZnO microrods, inset is an enlarged SEM image of an individual ZnO microrod. (b) PL spectrum of ZnO microrods excited by 325 nm laser. (c, d) Raman spectra of (c) the monolayer graphene on a 300 nm SiO_2-coated Si substrate and (d) an individual ZnO microrod.

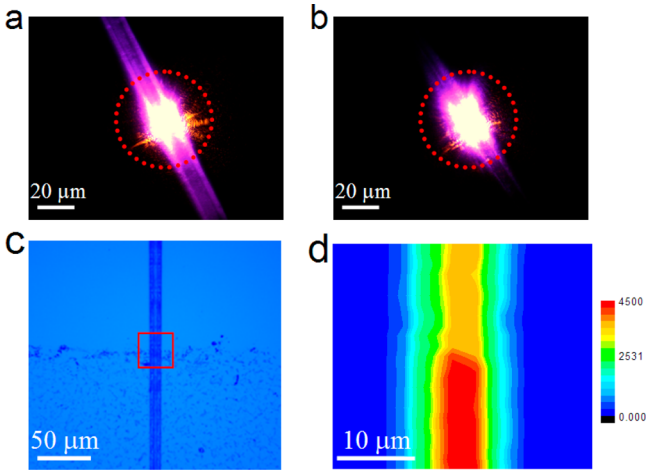

Figure 5. (a, b) Optical images of an individual ZnO microrod (a) before and (b) after graphene covering under the same excitation power of 325 nm laser. (c) Optical image of a ZnO microrod partially covered with graphene. (d) The micro-PL mapping image taken from the red rectangular region marked in (c).

Graphene induced PL enhancement was further investigated by micro-PL mapping. Figure 5c shows an optical image of a ZnO microrod partially covered with graphene, and Figure 5d shows the micro-PL image collected from the adjacent region with and without graphene covering and taken from the red rectangular region marked in Figure 5c. It exhibits clearly that the UV emission from the graphene-coated part is much stronger than that from the bare part.

Panels a and b in Figure 6 show the temporal-spectral images of the bare and the graphene-coated ZnO microrods, respectively. The comparison of the two images clearly demonstrates a much faster decay rate of the graphene-coated microrods than that of the bare ones. The TRPL spectra in Figure 6c is collected from the temporal-spectral images at probe wavelength of 393 nm. The results demonstrate two advantages of the graphene-coated microrods relative to the bare ones: (1) the emission intensity is about 3.5 fold stronger, agreeing well with the PL enhancement observed in Figure 5, and (2) the decay time becomes shorter. The effective PL lifetimes calculated from the normalized TRPL spectra have values of 16 and 23 ps, for the ZnO microrods coated with and without graphene, respectively. This indicates more efficient recombination of the excited carriers in the graphene-coated ZnO microcavity.

Above investigations have demonstrated the confined optical field and the enhanced UV emission from the graphene-coated ZnO microrod due to the effective coupling between graphene SP and ZnO interband emission. As aforementioned, the hexagonal ZnO microrod is favorable for the occurrence of WGM lasing due to the light multiple total internal reflection at the inner walls. Here, as a functional application, the graphene SP and corresponding physical effects were further applied to a hexagonal ZnO microrod to improve its WGM lasing performance. For comparison, three types of microcavities based on the same ZnO microrod were fabricated. Type I is the bare ZnO microrod, Type II is the microcavity in which graphene contacts one surface of the ZnO microrod, and Type III is the microcavity where graphene contacts the ZnO microrod on both the top and bottom surfaces.

Figure 7a–c shows the PL spectra of the three types of microcavities. Each sample presents a broad spontaneous emission at low excitation power density and converts definitely

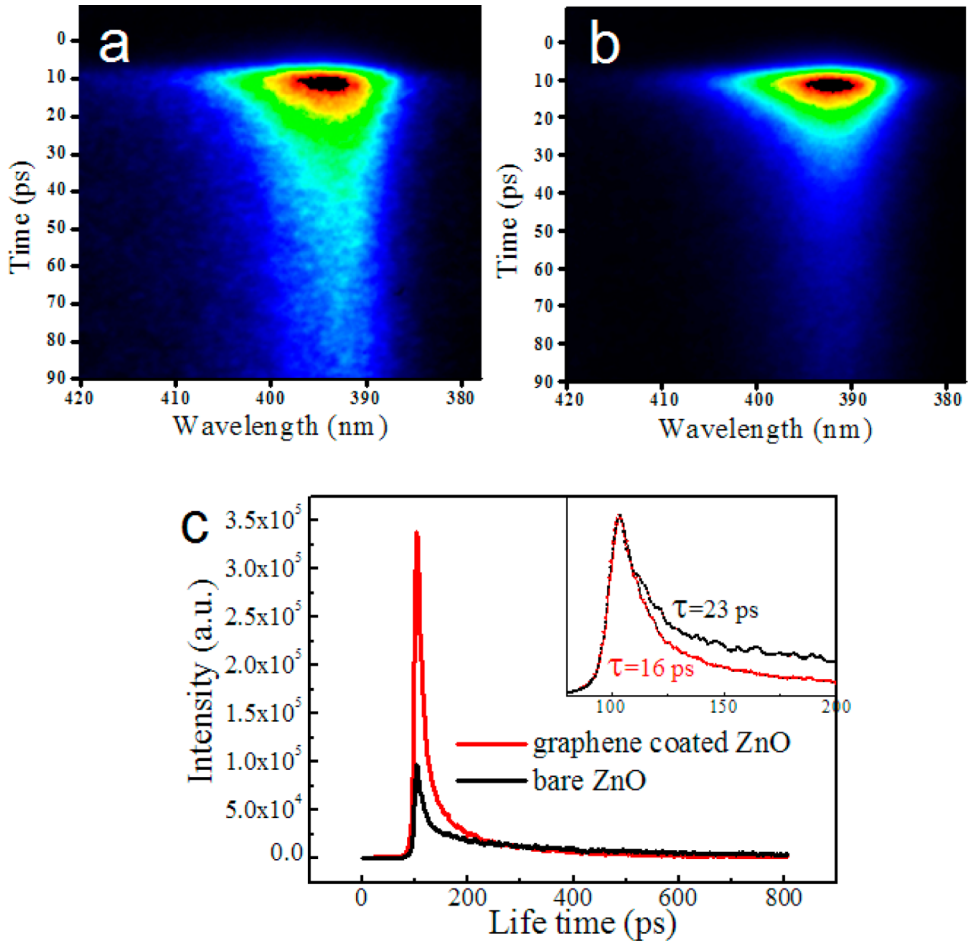

Figure 6. (a, b) Temporal spectroscopic profile of (a) the bare and (b) the graphene-coated ZnO microrods excited by 295 nm laser and collected by a streak camera. (c) TRPL spectra at the probe wavelength of 393 nm, inset is the normalized TRPL spectra.

into stimulated emission with distinct mode structures over a proper threshold. The definite threshold, sharp peaks and the superlinear increased intensity vs excitation power density confirm the lasing action in the microcavities. For type I, the threshold is estimated as 110 KW/cm^2 according to the PL spectra in Figure 7a. For the strongest mode at wavelength of 392.7 nm, the fwhm is about 0.08 nm, and the quality factor (Q) is calculated as about 4900 according to the equation, $Q = (\lambda/\delta\lambda)$, where λ and $\delta\lambda$ are the lasing mode wavelength and its fwhm, respectively. The experimental mode spacing matches well with the calculated value according to the equation of mode spacing for WGM cavity: $\Delta\lambda = (\lambda^2/[L(n - (\lambda\, dn/d\lambda))])$, where L is the path length of a round trip, n is the refractive index of ZnO, and $(dn/d\lambda)$ is the dispersion relation. In fact, the WGM mechanism has been discussed in our series reports previously.[22,23,26]

Panels b and c in Figure 7 show a similar evolution process from spontaneous emission to stimulated ones for type II and type III with increasing of the pumping power densities. The lasing peaks of the two types are much more pronounced and narrower than those of type I. The thresholds for type II and type III are about 80 and 50 KW/cm^2, respectively, which are much lower than that of type I. Meanwhile, the Q factor is increased to about 6000 for type II and about 6500 for type III. So it reveals the unambiguously improved lasing performance when the ZnO microrod was coated with graphene.

Furthermore, remarkably enhanced lasing intensity has also been achieved when the ZnO microrod was coated with graphene. Figure 7d shows the lasing intensity as a function of excitation power density for three types of microcavities. With increasing of the excitation power densities, the spontaneous emission intensity increases slowly below their respective threshold, and then rises up rapidly above the thresholds. It should be noted that the lasing intensity of type III increases more quickly than that of type II, which also increases more quickly than that of type I. This indicates the more efficient output of the hybrid microcavities than that of the bare one because of graphene SP-induced optical field confinement and corresponding effective coupling with ZnO. As more ZnO surfaces contact with graphene, more efficient coupling between graphene SP and ZnO interband emission would happen, resulting in the higher emission intensity of type III than that of type II.

4. CONCLUSIONS

In summary, the theoretical simulation on the graphene coated ZnO model demonstrated obvious optical field confinement due to graphene SP coupling into ZnO, and predicted the stronger light-matter interaction and enhancement of ZnO emission. In experiment, hybrid microcavities were fabricated by coating monolayer graphene on an individual ZnO microrod. Distinct optical field confinement and PL enhancement were observed intuitively, consistent with the theoretical

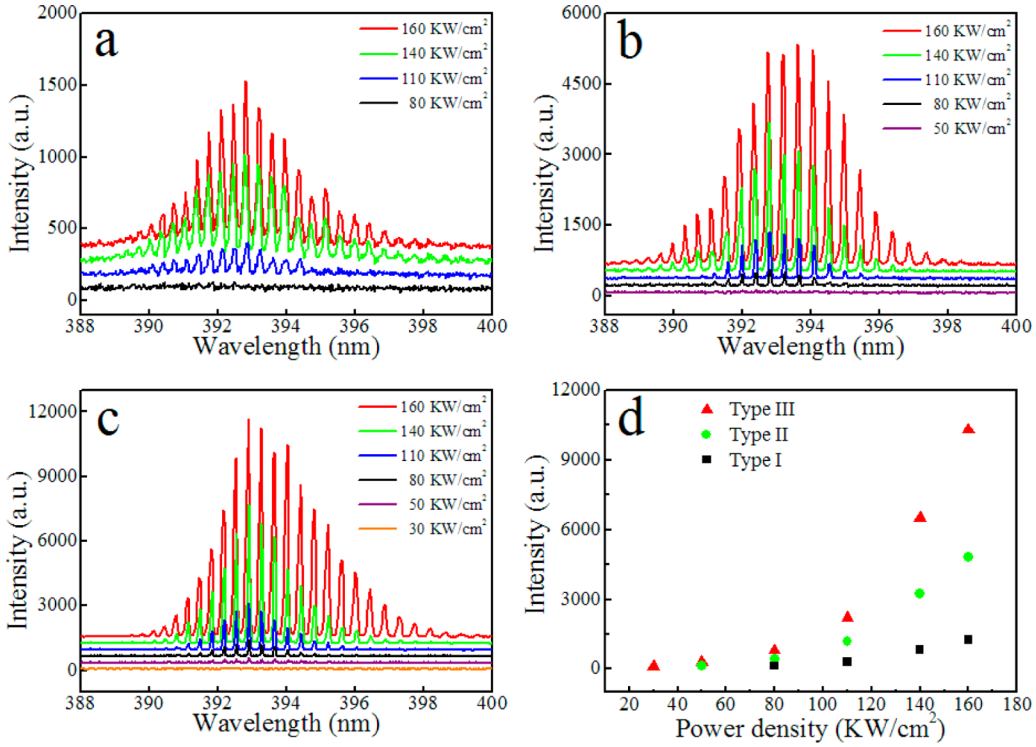

Figure 7. (a–c) Excitation power-density-dependent PL spectra of three types of microcavities: (a) type I, (b) type II, and (c) type III. (d) Correlation between emission intensities and excitation power densities for three types of microcavities.

simulations. TRPL experiments revealed the accelerated dynamics for the coupling process and indicated more effective recombination process in the graphene coated microcavities. As a functional application, the improved WGM lasing performance was realized. It demonstrated stronger lasing intensity, lower threshold, and higher Q factor as the bare ZnO microrod was coated with graphene. This investigation would be valuable for offering an efficient and controllable interface between nanoscale optics and electronics, also for designing novel optical and photoelectronic devices based on graphene–semiconductor hybrid materials, as well as holding great promise for a new generation of graphene-based optoelectronic devices, such as nanolaser, that break through the optical diffraction limit.

AUTHOR INFORMATION

Corresponding Author

*E-mail: xcxseu@seu.edu.cn.

Notes

The authors declare no competing financial interest.

ACKNOWLEDGMENTS

This work is supported by "973" Program (2011CB302004 and 2013CB932903), NSFC (61275054, 11104026, and 61376104), MOE (20110092130006), and JSIS (BE2012164).

REFERENCES

(1) Barnes, W. L. Light-Emitting Devices - Turning the Tables on Surface Plasmons. *Nat. Mater.* **2004**, *3*, 588–589.

(2) Ambati, M.; Nam, S. H.; Ulin-Avila, E.; Genov, D. A.; Bartal, G.; Zhang, X. Observation of Stimulated Emission of Surface Plasmon Polaritons. *Nano Lett.* **2008**, *8*, 3998–4001.

(3) Tsang, J. C.; Kirtley, J. R.; Bradley, J. A. Surface-Enhanced Raman-Spectroscopy and Surface-Plasmons. *Phys. Rev. Lett.* **1979**, *43*, 772–775.

(4) Huang, X. H.; El-Sayed, I. H.; Qian, W.; El-Sayed, M. A. Cancer Cells Assemble and Align Gold Nanorods Conjugated to Antibodies to Produce Highly Enhanced, Sharp, and Polarized Surface Raman Spectra: A Potential Cancer Diagnostic Marker. *Nano Lett.* **2007**, *7*, 1591–1597.

(5) Chen, L. M.; Luo, L. B.; Chen, Z. H.; Zhang, M. L.; Zapien, J. A.; Lee, C. S.; Lee, S. T. ZnO/Au Composite Nanoarrays As Substrates for Surface-Enbanced Raman Scattering Detection. *J. Phys. Chem. C* **2010**, *114*, 93–100.

(6) Tang, H.; Meng, G.; Huang, Q.; Zhang, Z.; Huang, Z.; Zhu, C. Arrays of Cone-Shaped ZnO Nanorods Decorated with Ag Nanoparticles as 3D Surface-Enhanced Raman Scattering Substrates for Rapid Detection of Trace Polychlorinated Biphenyls. *Adv. Funct. Mater.* **2012**, *22*, 218–224.

(7) Polman, A. Applied Physics Plasmonics Applied. *Science* **2008**, *322*, 868–869.

(8) Atwater, H. A.; Polman, A. Plasmonics for Improved Photovoltaic Devices. *Nat. Mater.* **2010**, *9*, 205–213.

(9) Novotny, L.; van Hulst, N. Antennas for Light. *Nat. Photonics* **2011**, *5*, 83–90.

(10) Okamoto, K.; Niki, I.; Shvartser, A.; Narukawa, Y.; Mukai, T.; Scherer, A. Surface-Plasmon-Enhanced Light Emitters Based on InGaN Quantum Wells. *Nat. Mater.* **2004**, *3*, 601–605.

(11) Lai, C. W.; An, J.; Ong, H. C. Surface-Plasmon-Mediated Emission from Metal-Capped ZnO Thin Films. *Appl. Phys. Lett.* **2005**, *86*, 251105.

(12) Lin, J. M.; Lin, H. Y.; Cheng, C. L.; Chen, Y. F. Giant Enhancement of Bandgap Emission of ZnO Nanorods by Platinum Nanoparticles. *Nanotechnology* **2006**, *17*, 4391–4394.

(13) Su, Y.-H.; Ke, Y.-F.; Cai, S.-L.; Yao, Q.-Y. Surface Plasmon Resonance of Layer-by-Layer Gold Nanoparticles Induced Photoelectric Current in Environmentally-Friendly Plasmon-Sensitized Solar Cell. *Light: Sci. Appl.* **2012**, *1*, e14.

(14) Krasavin, A. V.; Zayats, A. V. Passive Photonic Elements Based on Dielectric-Loaded Surface Plasmon Polariton Waveguides. *Appl. Phys. Lett.* **2007**, *90*, 211101.
(15) Gupta, R.; Dyer, M. J.; Weimer, W. A. Preparation and Characterization of Surface Plasmon Resonance Tunable Gold and Silver Films. *J. Appl. Phys.* **2002**, *92*, 5264−5271.
(16) Koppens, F. H. L.; Chang, D. E.; de Abajo, F. J. G. Graphene Plasmonics: A Platform for Strong Light-Matter Interactions. *Nano Lett.* **2011**, *11*, 3370−3377.
(17) West, P. R.; Ishii, S.; Naik, G. V.; Emani, N. K.; Shalaev, V. M.; Boltasseva, A. Searching for Better Plasmonic Materials. *Laser Photonics Rev.* **2010**, *4*, 795−808.
(18) Grigorenko, A. N.; Polini, M.; Novoselov, K. S. Graphene Plasmonics. *Nat. Photonics* **2012**, *6*, 749−758.
(19) Nair, R. R.; Blake, P.; Grigorenko, A. N.; Novoselov, K. S.; Booth, T. J.; Stauber, T.; Peres, N. M.; Geim, A. K. Fine Structure Constant Defines Visual Transparency of Graphene. *Science* **2008**, *320*, 1308−1308.
(20) Hwang, E. H.; Sensarma, R.; Das Sarma, S. Plasmon-Phonon Coupling in Graphene. *Phys. Rev. B* **2010**, *82*, 195406.
(21) Dubinov, A. A.; Aleshkin, V. Y.; Mitin, V.; Otsuji, T.; Ryzhii, V. Terahertz Surface Plasmons in Optically Pumped Graphene Structures. *J. Phys-Condens. Mater.* **2011**, *23*, 145302.
(22) Zhu, G. P.; Xu, C. X.; Zhu, J.; Lv, C. G.; Cui, Y. P. Two-Photon Excited Whispering-Gallery Mode Ultraviolet Laser from an Individual ZnO Microneedle. *Appl. Phys. Lett.* **2009**, *94*, 051106.
(23) Dai, J.; Xu, C. X.; Zheng, K.; Lv, C. G.; Cui, Y. P. Whispering Gallery-Mode Lasing in ZnO Microrods at Room Temperature. *Appl. Phys. Lett.* **2009**, *95*, 241110.
(24) Chen, R.; Ling, B.; Sun, X. W.; Sun, H. D. Room Temperature Excitonic Whispering Gallery Mode Lasing from High-Quality Hexagonal ZnO Microdisks. *Adv. Mater.* **2011**, *23*, 2199−2204.
(25) Gargas, D. J.; Toimil-Molares, M. E.; Yang, P. D. Imaging Single ZnO Vertical Nanowire Laser Cavities Using UV-laser Scanning Confocal Microscopy. *J. Am. Chem. Soc.* **2009**, *131*, 2125−2127.
(26) Zhu, G. Y.; Xu, C. X.; Cai, L. S.; Li, J. T.; Shi, Z. L.; Lin, Y.; Chen, G. F.; Ding, T.; Tian, Z. S.; Dai, J. Lasing Behavior Modulation for ZnO Whispering-Gallery Microcavities. *ACS Appl. Mater. Interfaces* **2012**, *4*, 6195−6201.
(27) Cheng, C. W.; Sie, E. J.; Liu, B.; Huan, C. H. A.; Sum, T. C.; Sun, H. D.; Fan, H. J. Surface Plasmon Enhanced Band Edge Luminescence of ZnO Nanorods by Capping Au Nanoparticles. *Appl. Phys. Lett.* **2010**, *96*, 071107.
(28) Lawrie, B. J.; Haglund, R. F.; Mu, R. Enhancement of ZnO Photoluminescence by Localized and Propagating Surface Plasmons. *Opt. Express* **2009**, *17*, 2565−2572.
(29) Cheng, P. H.; Li, D. S.; Yuan, Z. Z.; Chen, P. L.; Yang, D. R. Enhancement of ZnO Light Emission via Coupling with Localized Surface Plasmon of Ag Island Film. *Appl. Phys. Lett.* **2008**, *92*, 041119.
(30) Hwang, S. W.; Shin, D. H.; Kim, C. O.; Hong, S. H.; Kim, M. C.; Kim, J.; Lim, K. Y.; Kim, S.; Choi, S.-H.; Ahn, K. J.; Kim, G.; Sim, S. H.; Hong, B. H. Plasmon-Enhanced Ultraviolet Photoluminescence from Hybrid Structures of Graphene/ZnO Films. *Phys. Rev. Lett.* **2010**, *105*, 127403.
(31) Liu, R.; Fu, X. W.; Meng, J.; Bie, Y. Q.; Yu, D. P.; Liao, Z. M. Graphene Plasmon Enhanced Photoluminescence in ZnO Microwires. *Nanoscale* **2013**, *5*, 5294−5298.
(32) Cheng, S. H.; Yeh, Y. C.; Lu, M. L.; Chen, C. W.; Chen, Y. F. Enhancement of Laser Action in ZnO Nanorods Assisted by Surface Plasmon Resonance of Reduced Graphene Oxide Nanoflakes. *Opt. Express* **2012**, *20*, A799−A805.
(33) Dai, J.; Xu, C. X.; Sun, X. W. ZnO-Microrod/p-GaN Heterostructured Whispering-Gallery-Mode Microlaser Diodes. *Adv. Mater.* **2011**, *23*, 4115−4119.
(34) Li, X.; Cai, W.; An, J.; Kim, S.; Nah, J.; Yang, D.; Piner, R.; Velamakanni, A.; Jung, I.; Tutuc, E.; Banerjee, S. K.; Colombo, L.; Ruoff, R. S. Large-Area Synthesis of High-Quality and Uniform Graphene Films on Copper Foils. *Science* **2009**, *324*, 1312−1314.
(35) Jablan, M.; Buljan, H.; Soljačić, M. Plasmonics in Graphene at Infrared Frequencies. *Phys. Rev. B* **2009**, *80*, 245435.
(36) Ni, Z.; Wang, Y.; Yu, T.; Shen, Z. Raman Spectroscopy and Imaging of Graphene. *Nano Res.* **2010**, *1*, 273−291.
(37) Yu, T.; Ni, Z. H.; Du, C. L.; You, Y. M.; Wang, Y. Y.; Shen, Z. X. Raman Mapping Investigation of Graphene on Transparent Flexible Substrate: The Strain Effect. *J. Phys. Chem. C* **2008**, *112*, 12602−12605.
(38) Wang, R. C.; Liu, C. P.; Huang, J. L.; Chen, S. J. ZnO Symmetric Nanosheets Integrated with Nanowalls. *Appl. Phys. Lett.* **2005**, *87*, 053103.